Soil Dynamics and Earthquake Engineering 96 (2017) 89–103

Contents lists available at ScienceDirect

Soil Dynamics and Earthquake Engineering

journal homepage: www.elsevier.com/locate/soildyn

Safe distance of cultural and historical buildings from subway lines

Javad Sadeghi*, M. Hassan Esmaeili

Iran University of Science and Technology, Tehran, Iran

ARTICLE INFO

Keywords:
Monumental buildings
Safe distance
Vibration
Subway
Soil media

ABSTRACT

Construction and operation of subways (metros) closed to historical sites have been one of the main concerns of the world heritage protection bodies such as UNESCO. While metros alleviate condense traffic conditions and boost the tourism industry, the metro induced vibrations might damage cultural and historical structures (CHS). Although there have been various studies into the metros vibration characteristics and the CHS protection methods, there is still a lack of sufficient investigations into the measures by which a safe distance of the CHS to the metro can be derived. In response to this need, a thorough theoretical and experimental investigation was made in this research, aiming at developing a safe distance prediction graphs (SD). For this purpose, a finite element model of the track and the surrounding media was developed. The advantage of the model over the current ones is the consideration of the real (in situ) train loading conditions as an input. The model was validated by comparisons of its results with those of a comprehensive field measurement carried out in this research. New classifications of the CHSs and the track sub-structure form the aspect of metro-induced vibrations were developed in this research. Through parametric analyses of the model, the SD was developed for the first time as a function of metro characteristics, geo-mechanical properties of the media between the metro and the CHS, and the type of CHS. The effectiveness and practicability of the SD in construction of new subway lines were illustrated. It was shown that the SD graphs developed here can be taken as an effective tool for the design of subway lines in historical cities.

1. Introduction

One of the most important challenges in the construction and operation of urban railways (particularly subways) is the possibility of railway damages to the neighboring structures, in particular monumental buildings. A recent report released by the Iran Cultural Heritage, Handcraft and Tourism Organization (ICHTO), indicates that severity of the damages to the historical structures due to the construction and operation of metros has been one of the main problems in the preservation of monumental structures in the Iranian historical cities [1].

There are noticeable increases in construction of rail infrastructures in the cosmopolitan cities, particularly in the Asian and Meade-East countries where there are many cities with considerable number of residential and monumental structures [1,2]. Although a subway system is a safer, more economical and faster system of transportation (compared to the other systems) and in turn, boost the tourism industry [3,4], the Long-term metro induced vibrations might seriously damage historical structures due to low-intensity steady vibrations [5–7].

In the last three decades, considerable number of investigations have been conducted on the behavior of the CHS under the vibrations from various sources including explosion [8,9], road traffic [10–12] and construction machineries [13,14]. Results of investigations have been compared with various allowable vibration levels to evaluate the building safety [15]. It has been shown that the vibrations of small amplitude characterized by a high number of cycles may cause deterioration of mortar, its detachment from the bricks and consequently reduction of masonry strength [16–18].

However, less attention has been paid to the effects of metro vibrations on the CHS [19]. The only serious research have been made by Ma et al. who focused on evaluating train vibration impact on a historic bell tower above two metro lines in China [19]. The majority of related investigations on protection of CHS from railway vibrations are limited to the mitigation of the vibrations at the source. For instance, Federal Transportation Association (FTA) has used a hybrid semi-empirical approach to investigate the railway vibration received by the surrounding structures and presented several mitigation measures for subway superstructure in the form of guidelines [20]. Vogiatzis and Kouroussis used the finite element modeling technique and in-situ measurements of floating slab tracks in the Athens Metro to evaluate the effectiveness of the floating slabs in reduction of the effects of the

* Corresponding author.
E-mail addresses: javad_sadeghi@iust.ac.ir (J. Sadeghi), m_h_esmaily@rail.iust.ac.ir (M.H. Esmaeili).

http://dx.doi.org/10.1016/j.soildyn.2017.02.008
Received 30 September 2016; Received in revised form 6 January 2017; Accepted 25 February 2017
Available online 07 March 2017

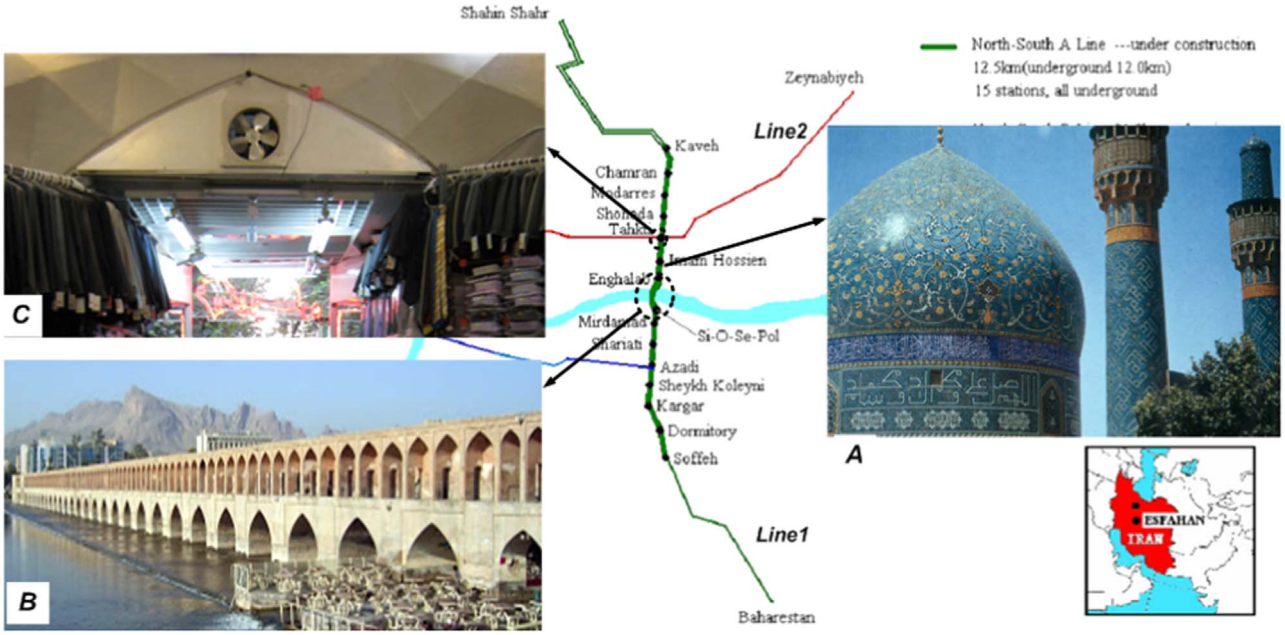

Fig. 1. Monumental buildings closed to line 1 of Isfahan subway, A) MCC; B) SSP and C) SKH.

Fig. 2. Instrumented monumental buildings to measure vibration received by historical structures using FTA method, A: MCH, B: SSP.

environmental induced vibrations on various high cultural value buildings along the given Athens Metro Extensions [21,22]. Cox and Wang made experimental studies to examine the effectiveness of different fastening and slab-track systems on the reduction of track vibration levels [23]. However, there is a need for a measure by which the safety of the CHS can be evaluated and in turn, the safe Metro-CHS distance for each type of subway superstructure, soil media properties, and various CHS categories can be derived/predicted. A review of the available literature indicates that there isn't any regulation or guideline for the safe Metro-CHS distance [19,24].

In response to this need, a comprehensive theoretical and experimental investigation was made in this research, leading to develop a

Table 1
Comparison of subway vibration received by three monumental structures with the allowable limits.

Location	PPV (mm/s)	Allowable limits (velocity, mm/s)
SSP	0.33	0.25
MCH	0.29	0.15
SKH	0.4	1

Table 2
Classification of track structures based on their stiffness and loss factors.

NO	ID	Description	Track Stiffness (kN/mm/m)	Loss factor (2*ζ)
1	FST-ML	Mat – Low stiffness	5	0.5
2	HRF	High Resilient Fasteners [Vanguard, Pandrol CDM]	5.3	0.3
3	HSS	Helical Steel Springs	5.5	0.02
4	FST-SL	Strips – Low stiffness	6.4	0.5
5	FST-SM	Strips – Medium stiffness	8	0.5
6	FST-PL	Pad – Low stiffness	10	0.5
7	MRF	Medium Resilient Fastener [Colon egg]	10	0.02
8	FST-MH	Mat – High stiffness	11	1
9	FST-SH	Strips – High stiffness	13.5	0.5
10	FST-MM	Mat – Medium stiffness	25	1
11	DFT-RP1	Simple fastener with soft pad	35	0.1
12	DFT-RP2	Simple fastener with stiff pad	55	0.07
13	DFT-RP3	Simple fastener with high stiff pad	72	0.1

Table 3
Soil classifications.

Class	Description of material	S-wave velocity (m/s)
A	Rock	≥750
B	Very dense soil and loose rock	360–750
C	Stiff soil	180–360
D	Soft soil	≤180

Metro-CHS safe distance graphs. The graphs provides the safe distance based on the type of metro structural properties, the geo-mechanic properties of the media (between the metro and the CHS), and the type of the CHS. In this paper, first, the importance and the necessity of this research were illustrated by discussing the results of a filed investigation on the effects of metro vibrations on historical structures. Then, a finite element model of metro system and surrounding media was developed and validated thorough a compressive field investigation. Finally, the Safe Distance (SD) was developed by conducting a parametric analysis of the model. The effectiveness of the graphs was evaluated by applying the graphs in a historical city.

2. Description of problem

To investigate the possibility and the extent of metro vibrations damages to the historical structure and the effectiveness of the current technique in protection of CHSs, a prior filed investigation was made in this research in the old city of Isfahan which is one of the historical cities registered by UNESCO [1]. The central part of this city has several beautiful masques and churches, old palaces, historical bridges and several monumental buildings. Isfahan subway goes through "Charbagh Avenue" in the central part of the city in which there are several nationally and internationally registered historical monuments including "Si-o-Se-Pol (SSP), (a thirty-three arches bridge built in 700 years ago), Madreseh-Charbagh (MCH) (a historical school built 600 years ago) and SarDar-E-KHeymeghah (SKH) (a 400 years old building). MCH, SSP and SKH are 26, 8 and 15 m away from the subway centerline (radial distance), respectively (Fig. 1). The field investigation encompassed three stages: instrumentation of monumental structures, recording the amount of vibrations received by the historical structures using the FTA method [20] (Fig. 2), and comparisons of the vibrations received by the CHSs with the allowable limits (Table 1). Note that the allowable limits were adapted from Asian standards (from China and Malaysia) which are the most appropriate standards based on the structural properties of the CHSs in Isfahan [25,26].

The results obtained from the field measurement are presented in Table 1. As indicated in this table, despite all the measures taken by the metro authorities for protection of the adjacent CHSs in the design and construction of Isfahan metro (Line 1), the vibrations received by all three CHSs exceed the allowable limits (up to 20–30%). This clearly indicates that the current design techniques would not ensure the safety of the CHSs. Furthermore, the level of metro vibrations considerably increases during the time because of the metro substructure degradation (such as growth of rail corrugation or deterioration of track damping system).

Monumental buildings have old masonries and therefore, if they are damaged, they cannot be easily repaired. Thus, keeping the metro line in a safe distance from the CHS is highly preferable.

3. Research methodology

This research is aiming at developing practical graphs for the minimum required distance between CHSs and subway lines. The graphs are to provide the safe distance as a function of the track structure, the surrounding soil properties and the CHS types. The criterion considered in this research is the maximum allowable vibration limits received by the CH structures in the decibel scale.

According to the literature, the vibration level received by monu-

Table 4
Various categories of monumental/historical structures.

Class	Structural type	Preservation level	Building facade	Allowable Vib. velocity, mm/s (dB)
I	Brick and mortar masonry	Provincial	–	1 (92)[a]
II	Brick and mortar masonry	National or international, Unesco registered	Without cosmetic or plaster	0.25 (80)[a]
III	Brick and mortar masonry	National or international, Unesco registered	With cosmetic or plaster	0.15 (75)[a]
IV	Stone masonry	National or international, Unesco registered	–	2 (95)[a]
V	Timber	National or international, Unesco registered	–	0.2 (78)[a]

[a] Vertical PPV.

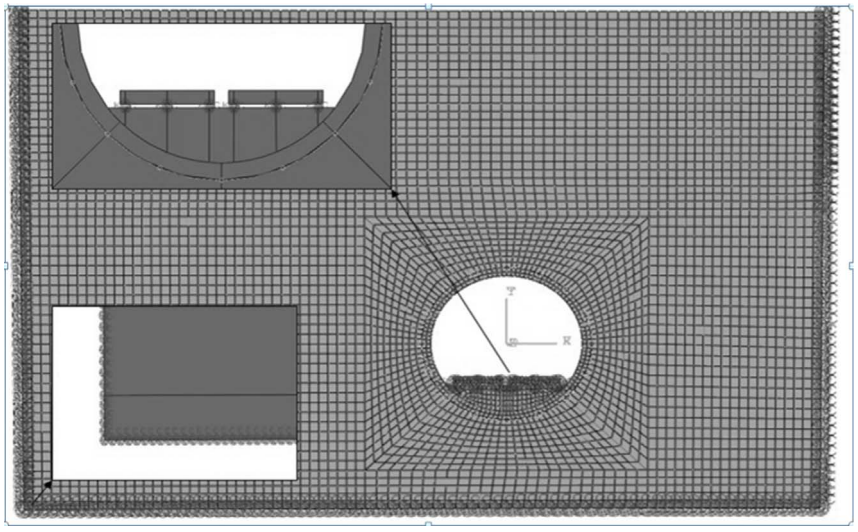

Fig. 3. FEM model geometry, Mesh and boundaries.

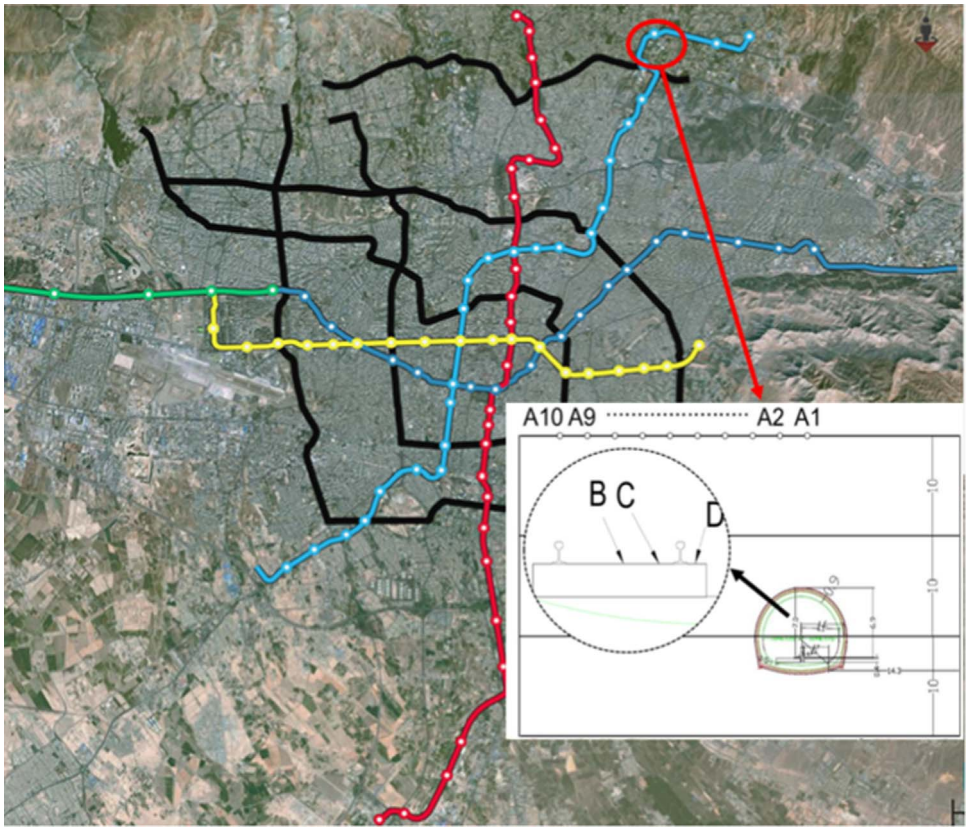

Fig. 4. Test location – Tehran Metro line 3.

mental structures is influenced by several sources including subway superstructure characteristics, the surrounding soil media dynamic properties, and the structural type of CHSs [20,27]. In order to make the results practical, the subway superstructure systems, the path or media between (soil layers) and, the CHSs were classified into certain groups, classes or categories. To classify the subway systems, all the available metro subsystems were studied [22,23,28–32], and as a result, they were divided into 13 categories based on their stiffness (varying from 5 to 72 MPa) and damping coefficients (Table 2). The stiffness and damping of each superstructure category were derived

Fig. 5. Field tests setup, (a) Ground surface vibration measurement, (b) Attachment of accelerometers on the slab track at points B–D, (c) Measuring of track acceleration, (d) Metro train used in the tests (e) Track deflection measurement, (f) LVDTs arrangement in track deflection measurement.

Table 5
Details of the train used in field tests.

Types	Center to center of axle in bogie (m)	Axial load (ton)	Car Length (m)	Max Speed (km/h)	Number of bogies for each train
DC-TC	2.7	14	19.52	100	28
AC-M[a]	2.7	10.5	20.1	100	28

[a] This type of train is considered as the reference.

from the literature.

The classification of the soil media between subways and CHSs were made based on the international seismic codes (Table 3) [33–36]. As given in Table 3, there are 4 classes of soil layers based on the shear speed of the wave in the soil layer. The shear wave speed was considered as the identification of the soil class [37].

In order to classify the monumental buildings, 13 relevant codes of practice (or standards) available in the literature [25,26,38–43] were studied, and consequently, the CHSs were classified into five groups based on their structural properties, preservation levels (provincial, national or international) and their façade conditions (Table 4). As indicated in this table, Classes *I*, *II* and *III* are made of brick and mortar, Class *IV* has rock and stone structures and Class *V* has timber structures. The main differences between Classes *I*, *II* and *III* are the importance of the structure and their façade conditions. Class *I* is not historical but contributes to the ancient shape of the historical sites.

Parametric analyses were made to investigate the effects of various influencing parameters on the vibration levels received by the CH structures. For this purpose, a 2.5D model including the subway tunnel and its surroundings media was developed. The model was validated based on the results obtained from the field tests carried out in the Tehran subway lines. The results obtained were analyzed, leading to drive guidelines graphs for the required minimum distance.

4. Development of model of track and surrounding media

The model comprises of a slab track super-structure (including the slab, the backfill concrete, and the elastic layer), and the surrounding soil (in two layers). The model was developed in a widely used finite element software (called ABAQUS) as its effectiveness and advantages have been shown in the literature [44,45]. According to the literature [46], the track components and the surrounding soil layers have linear

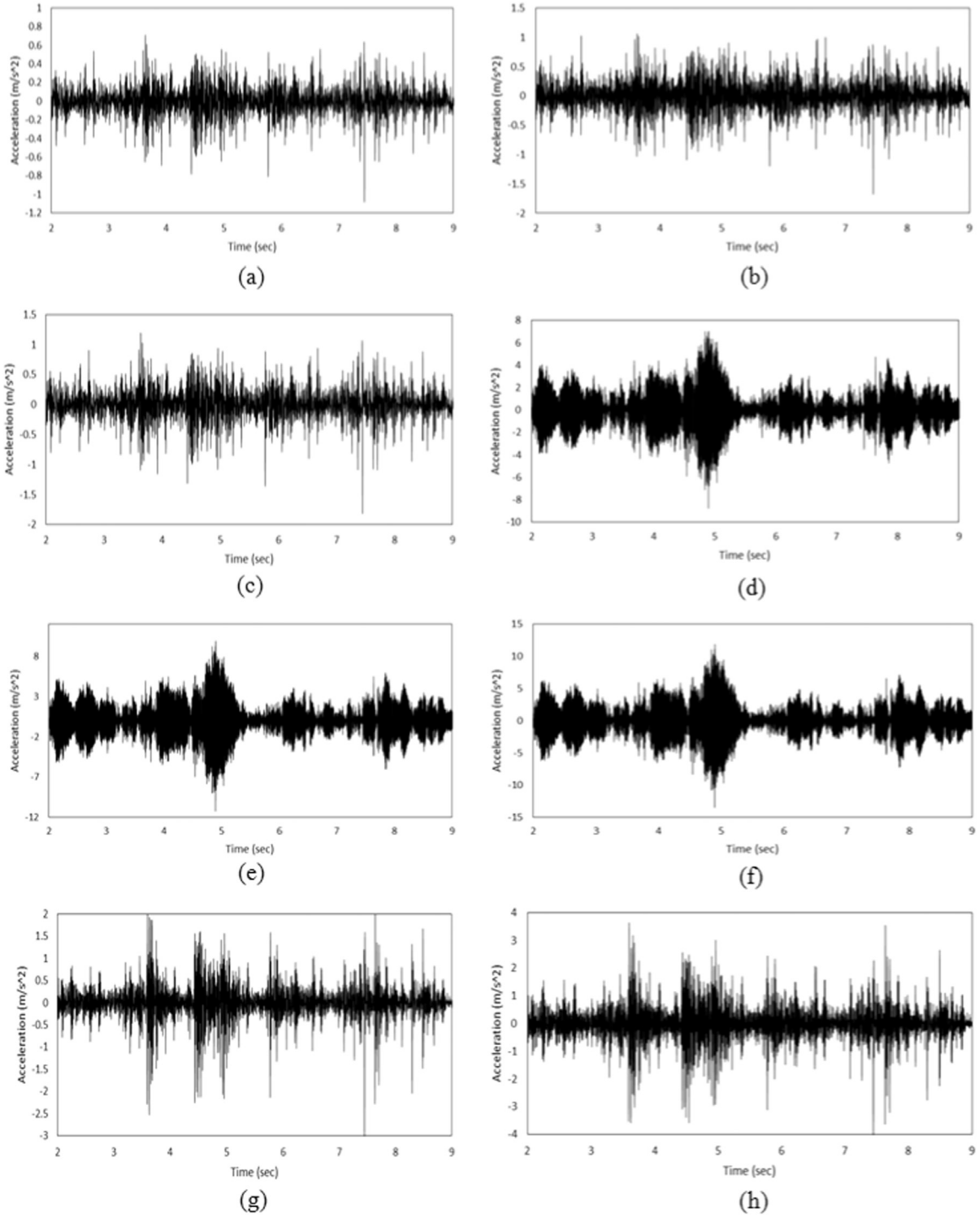

Fig. 6. Time history: track responses measured at Points B–D for speed range of 20–70 km/h, (a) at Point B, V=20 km/h, (b) at Point B, V=50 km/h, (c) at Point B, V=70 km/h, (d) at Point C, V=20 km/h, (e) at Point C, V=50 km/h, (f) at Point C, V=70 km/h, (g) at Point D, V=20 km/h, (h) at Point D, V=70 km/h.

mechanical behaviors in the vibration ranges of the track system. Therefore, all of the elements were considered to have an elastic mechanical behavior. Damping of the elements was obtained, using the method proposed by Rayleigh and Lindsay [47]. The Rayleigh damping for the soil was obtained from Eq. (1) as under:

$$C = \alpha[M] + \beta[K] \tag{1}$$

where $[M]$ is the mass matrix, $[K]$ is the stiffness matrix; and α and β are the mass and stiffness coefficients as derived from Eq. (2):

$$\begin{Bmatrix} \alpha \\ \beta \end{Bmatrix} = \frac{2\,\omega_i\,\omega_j}{\omega_j^{\,2} - \omega_i^{\,2}} \begin{bmatrix} \omega_j & \omega_i \\ -\frac{1}{\omega_j} & \frac{1}{\omega_i} \end{bmatrix} \begin{Bmatrix} \beta_i \\ \beta_j \end{Bmatrix} \tag{2}$$

Where the angular velocity (ω=2πf) and the subscripts i and j present the range of the analysis frequencies.

It is detailed in Fig. 3. The elements used in the model are plane

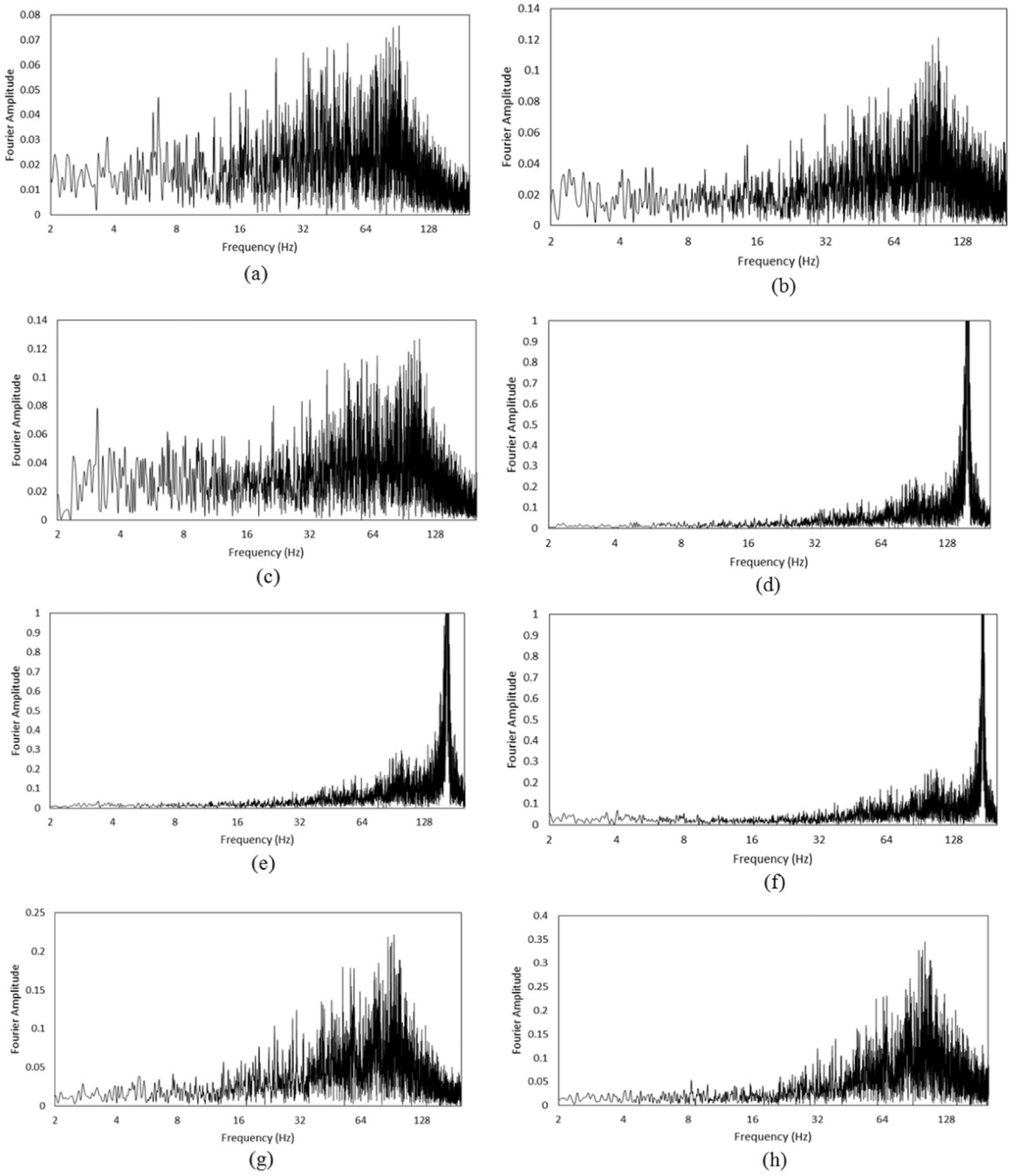

Fig. 7. Frequency contents of track responses measured at Points B–D for speed range of 20–70 km/h, (a) at Point B, V=20 km/h, (b) at point B, V=50 km/h, (c) at Point B, V=70 km/h, (d) at Point C, V=20 km/h, (e) at Point C, V=50 km/h, (f) at Point C, V=70 km/h, (g) at Point D, V=20 km/h, (h) at Point D, V=50 km/h.

strain solid elements named CPS4R. The slab, the backfill concrete, and the tunnel lining were modeled using 8-node solid elements. The elastic layers were modeled as discrete springs and dampers considered under the slab-track. The mesh used in the model is the "quad dominated sweep type" for soil and the "quad dominated free type" for the lining, the slab and the backfill concrete. The mesh sizes are 0.5, 0.25 and 0.2 m for the soil, the tunnel lining and the slab, respectively.

The real train loading conditions were taken into the model using a numerical modeling technique called 'secondary base motion method', in which the load considered as an acceleration time history applied to the train mass [48]. This was made by measuring acceleration time histories of the slab when the train passed over. This method leads to more accurate results when compared with the conventional method of driving the track loading pattern from the theoretical vehicles models such as multi-body mass system [44,49] or the load time history models [50]. In order to avoid elastic wave reflection, the tangential and normal viscous boundary conditions were used, based on the method described by Lysmer and Kuhlemeyer, and Kouroussis et al. [51,52].

5. Model validation

A through filed measurement was carried out in the Tehran subway network in order to validate the model. For this purpose, the results obtained from the field were compared with those of the model when

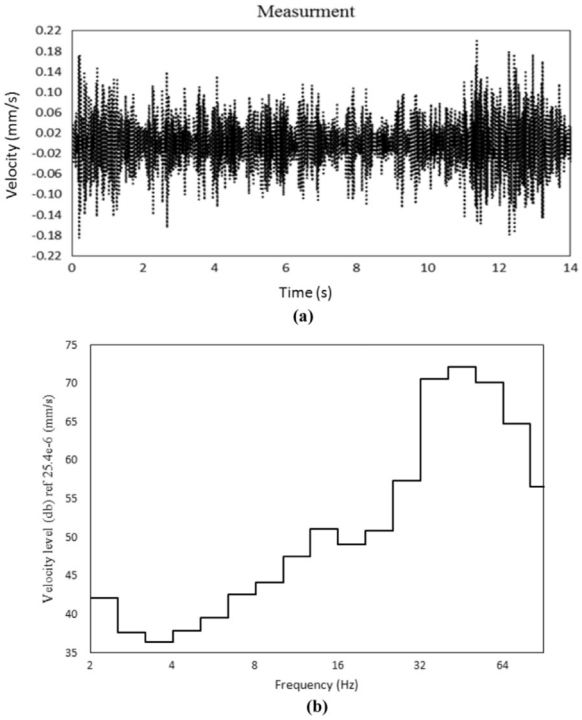

Fig. 8. Sample of vibration levels measured at the ground surface (at point A2) in: (a) Time domain; (b) Frequency domain.

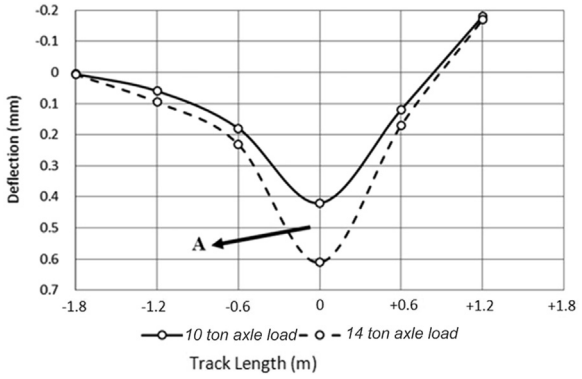

Fig. 9. Track deflection measured on 5 consequent sleepers.

all the properties of the field were taken into the model. They are described as under.

5.1. Field tests

The testing procedure was well studied before it commenced. It included the selection of the test fields, and the tests procedure (i.e., tests setting, instrumentations and method of data acquisition). As a result, the tests were carried out in the Tehran subway, Line 3 between Zeinodin and Ghaem stations. Fig. 4 presents the test locations. Measurements were taken in six consequent days. Recording were made from 13 points. Ten recording points were set on the ground

Table 6
Properties of track and tunnel elements (TUSC [58]).

	Element	Type	Poisson ratio	Density	Thickness	Modulus of elasticity
		-	-	kg/m^3	mm	MPa
1	Slab track	Rehda 2000	0.2	2400	400	30800
2	Tunnel invert backfill concrete	–	0.2	2400	300	22900
3	Tunnel lining	–	0.2	2400	350	30800

surface (Points A1–A10) and three points were selected closed to the track (Points B–D). A1–A10 are in radial distances of 21, 26, 35, 47, 55, 64, 73, 80, 91 and 97 m from the double track center line. These points cover all the locations which receive the most severe vibrations caused by the passing trains. The load time histories were measured by installing accelerometers on the top of the slab (Point B–D) and the responses were recorded form the assigned points at the ground (Points A1–A10) when the train passed with various speeds.

Three component compact molecular-electronic seismic velocity sensors were installed on the ground at Points A1–A10 to measure the vibrations of the ground surface in three directions (Fig. 5a). The sensors had the ability of working within 15° tilt relative to the vertical axis in order to eliminate the local ground inclinations. The sensitivity range of the sensors was up to 250 V s/m, with the maximum input signal of ± 30 mm/s, and the frequency range of 1–250 Hz which covers the interested ranges of railway environmental vibrations [53]. It has been shown that these sensors are capable of measuring low ground frequency micro-vibrations [54,55]. Geo-Arm digitizer with accuracy of 200 sample/s was connected to the sensor to convert the analog output signal to the input seismic signal (Fig. 5a). Three-axial accelerometers (type Sinocera CA-DR capacitance) with the frequency range of 0–400 Hz were installed at Points B–D and connected to a data logger by which the output accelerations were recorded (Fig. 5b and c). Accelerometers with an accuracy range of 1–10 m/s^2 were set on 3 points of the slab to derive the pattern of the slab surface accelerations. Accelerometers were selected, considering the possible range of track accelerations and working conditions. The application of these sensors is discussed in [56]. Data acquisition was made for 15 s for each train pass in order to record the data in a wide range. The acceleration time histories were recorded at the points when the trains run over the track (Fig. 5c). The typical metro trains (consisted of 7 cars) with the speed range of 10–80 km/h were used for the loading (Fig. 5d). The general specifications of the trains are presented in Table 5. The maximum axle load was 14 t. A series of LVDTs were mounted on the slab and fixed to the ground to measure the slab absolute deflections (vertical deflections of the slab track relative to the ground) (Fig. 5e). A view of the LVDTs installations are presented in Fig. 5e and f.

Fig. 6 presents the track acceleration time histories recorded at Points B–D for the train speeds varying from 20 to 70 km/h. As illustrated in this figure, the track response increases with the speed of the train. The frequency contents of the measured accelerations are presented in Fig. 7. As indicated in this figure, the amplitude is increased in the frequency range of 30–100 Hz, which is due to the rail unevenness. The dominant frequencies of subway system are approximately 32, 65 and 105 Hz for fastening, rail corrugation and Pin-Pin condition of the rail, respectively. This agrees with what have

Table 7
Specifications of soil layers in Line 3 stations W3-Y3 (TUSC [59]).

Depth m	*S wave speed* m/s	*P wave speed* m/s	*Poisson ratio* -	*Balk modulus* MPa	*Shear modulus* MPa	*Young modulus* MPa	*Density* gr/cm^3
0–0.05	480	820	0.24	584	369	914	1.6
0.5–4	540	920	0.24	755	481	1191	1.65
4–6	600	1040	0.25	1053	630	1576	1.75
6–10	700	1200	0.24	1416	882	2191	1.8
10–16	800	1370	0.24	1842	1152	2860	1.8
16–20	880	1500	0.24	2252	1433	3546	1.85
20–28	900	1560	0.25	2504	1499	3748	1.85

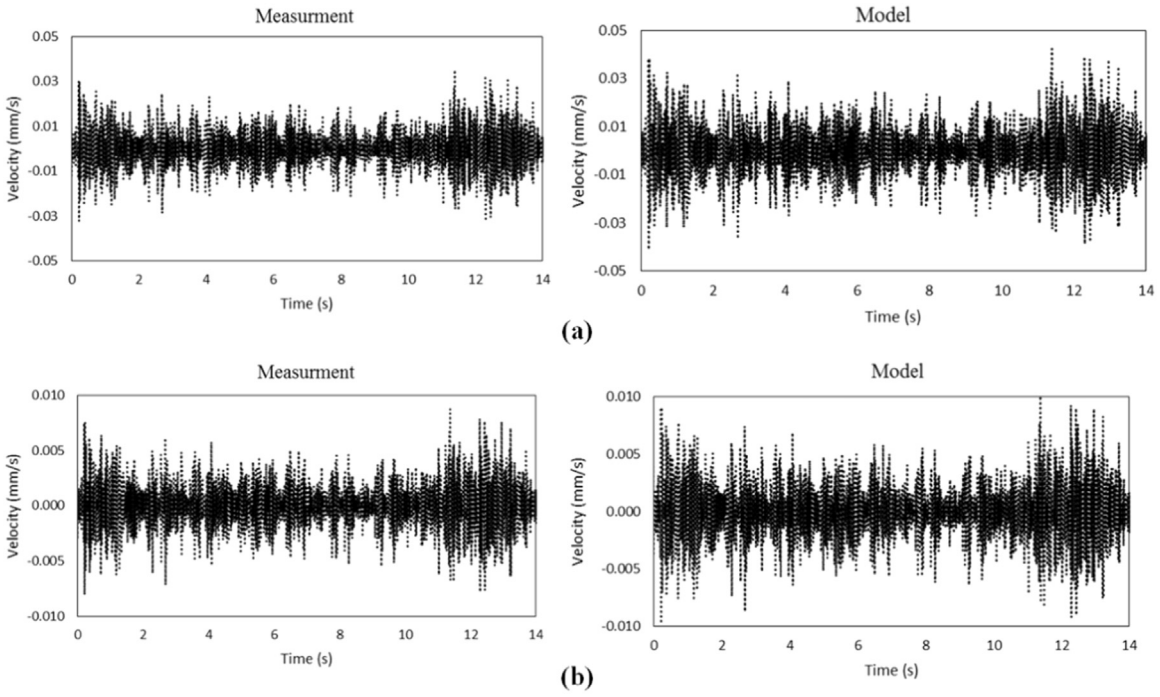

Fig. 10. Comparison of velocity time histories on the ground surface (a) Point A5 (b) Point A10.

been found in [57]. Fig. 8 presents the velocity time histories measured at Point A2. Similar measurements were also obtained for Points A1 and A3–A10. The track deflection measurements for 10 and 14 t axle loads are presented in Fig. 9.

5.2. Comparisons of results

The properties of the elements (including the slab, the tunnel invert backfill concrete, and the tunnel lining) used in the model are presented in Table 6. The data provided in this table were obtained from the tests reports released by the Tehran metro consulting companies [58]. Soil layers properties were derived from seismic tests made on the samples obtained from 5 boreholes with 30 m depth (drilled by the Tehran Metro contractors in 2013–2015 [59]). The properties of the soil layers are summarized in Table 7. According to Table 3, the first layer is composed of very dense soil (Class B) with 10 m thickness ($450 < Vs < 750$), and the second layer with the shear wave speed more than 750 m/s was identified as bedrock (Class A). Radial distance from double track centerline to the ground level is 18 m. The outer tunnel radius is 3 and the lining thickness is 35 cm. The specifications of the slab track, the tunnel system and the soil layers indicated in Tables 6 and 7 were considered in the model. The stiffness of the track was calculated using Talbot-Wasiutynski method [60]. This was made by dividing the amount of differences in the wheel loads by the area under the deflection curve (Fig. 9). As a result, the computed track stiffness was 71 MPa.

Two indicators were used to evaluate the validity of the model. They were the system energy (RMS) and the vibration level (PPV).

The train loads have complex mechanisms due to the wheel and rail unevenness, the local rail joint defects, the wheel flats [45], and the rail seat periodicity. Therefore the real train load was imported into the model based on the results obtained in the field measurements. That is, the train load was used in the model by considering the measured acceleration time histories (indicated in Fig. 6) at the slab model boundaries. Comparisons of the ground vibration levels at Points A5 and A10 are presented in Fig. 10. As indicated in this figure, the amounts of maximum velocity at Points A5 and A10 are 0.041 and 0.001 mm/s obtained from the model and 0.035 and 0.009 mm/s from

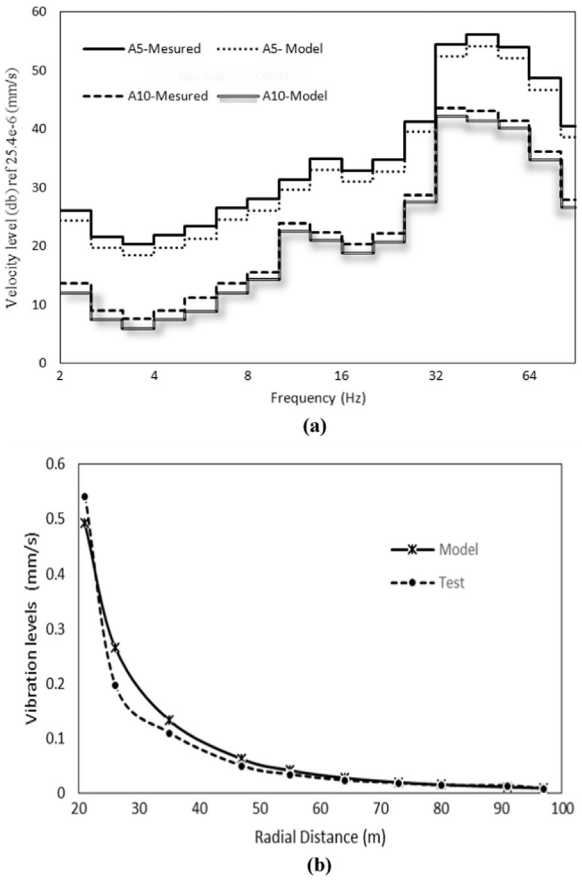

Fig. 11. Comparison of measurements and model predictions, (a) One-third octave band spectra for the vertical velocity level, (b) Pick Particle Velocity for A1–A10.

the measurements. This indicates a good level of agreement between the theoretical results and the measurements. The measured and calculated ground vibration levels in the 1/3 octave band frequency domain are also presented in Fig. 11(a). Due to the uncertainty in the sensor results in the frequencies less than 2 Hz, the comparisons are made for the frequencies higher than 2 Hz. As illustrated, the difference between the results in the frequency range of 2–100 Hz is 2.2 db (10%) which is reasonably low (acceptable). The comparison for other points at the ground level is presented in Fig. 11(b) which indicates a good level of agreement between theoretical and experimental results.

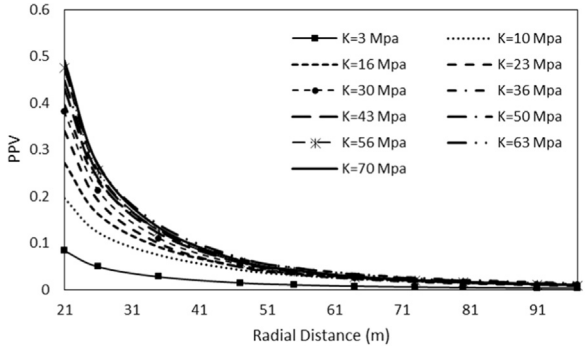

Fig. 12. Vibrations at recording points (A1–A10) for various types of track systems.

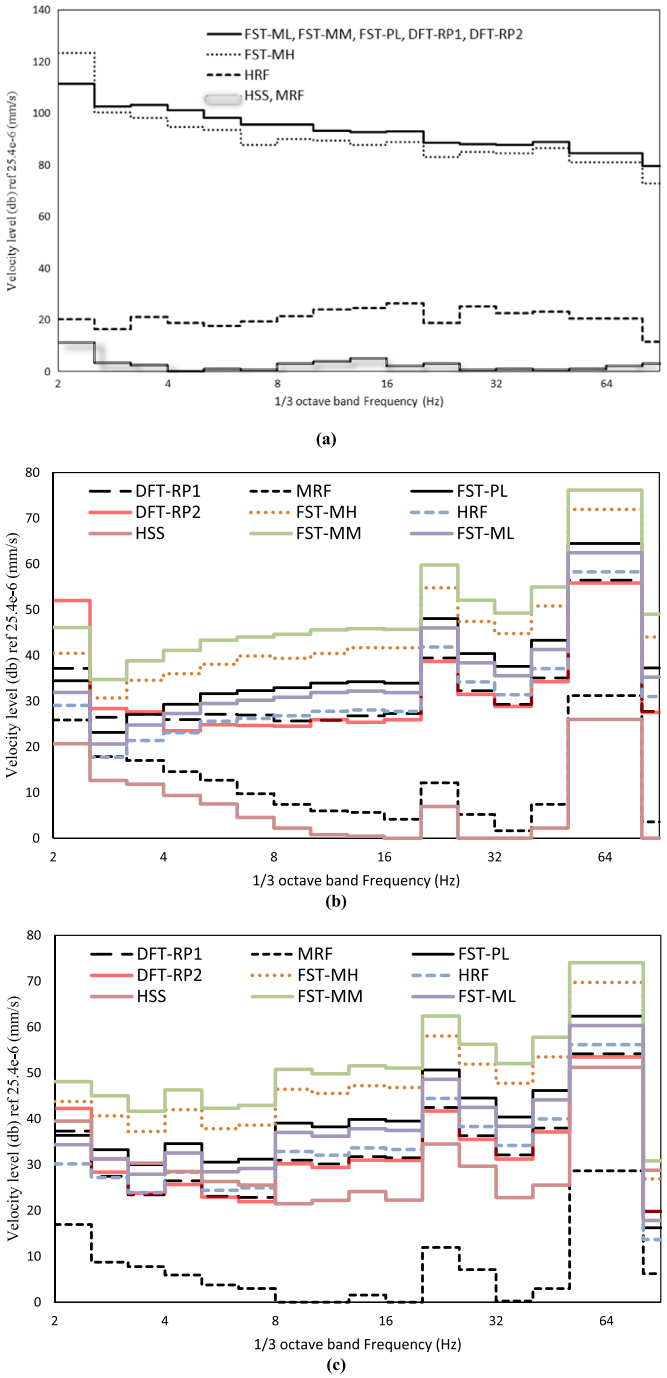

Fig. 13. Effect of subway superstructure types on track and ground vibration level in frequency domain (a) Close to the track at the tunnel invert, (b) On ground surface at tunnel head, (c) On ground surface (average).

6. Parametric analysis

The model was used in order to evaluate the influences of the track type, the properties of the soil media and the structural characteristics of the CHS on the vibration levels received at the CHS critical points. This is made by a comprehensive parametric analysis of the model, taking into consideration the classifications defined in Tables 2 and 3.

6.1. Subway structure

The vibrations (Peak Particle Velocity: PPV) at the recording points

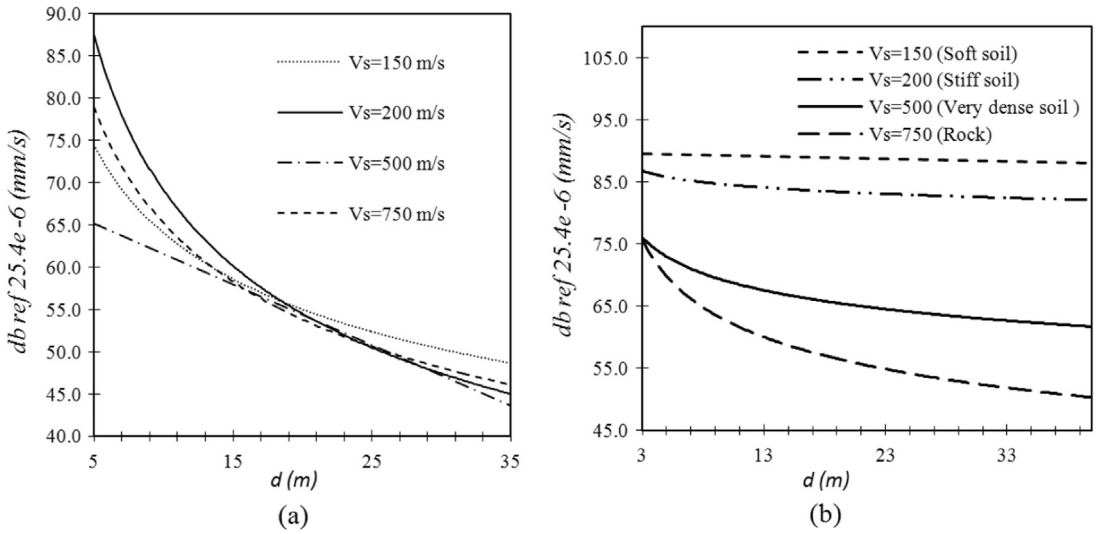

Fig. 14. Effect of soil variations in two layers on ground vibration level in various radial distance from track centerline (a) First layer (top), (b) Second layer (underneath).

(A1–A10) for different types of track systems (track stiffness) are presented in Fig. 12. As expected, this Figure indicates that vibration levels decreases in magnitude when the radial distance increases or the track stiffness decreases. The effect of track stiffness on vibration levels becomes less with increases of the distance from the load. The PPV becomes almost constant at the distances greater than 80 m.

The vibration levels in the frequency domain for various types of subway structure, closed to the track at the tunnel invert, on the tunnel head (Point A1) and its average on the ground (Point A1–A10) are plotted in Fig. 13a–c, respectively. As illustrated in these figures, the maximum vibration levels at the ground surface are in the frequencies range of 16–80 Hz, while in most cases, the maximum levels close to the track (at the tunnel invert) are in the frequencies less than 16 Hz. The vibration level at the ground is reduced as the vibration moves to the ground from the source (the track) especially for the frequencies less than 16 Hz (i.e., the soil layers works as a high pass filter). The results also indicate that the maximum vibration levels at the ground are at the frequencies of 30 and 64 Hz. Based on Fig. 13b and c, although the maximum reduction of vibrations was expected in the system with a minimum stiffness, the highest performance in vibration reduction was occurred in the system with the lowest damping coefficient (i.e. HSS, MRF, DFT-RP2 and DFT-RP1 with damping coefficient of 0.01, 0.01, 0.035 and 0.05). This indicates the importance of considering damping coefficient along with system stiffness.

6.2. Soil media properties

The ground vibration levels versus the radial distance from the track centerline (varying from 5 to 100 m (for the first and the second layers are plotted in Fig. 14. This figure presents the vibration levels for all four classes of the soil defined in Table 2. It is apparent form this figure that shear wave speed changes have considerable effect on the ground vibration level. Attenuation rate is more in the stiff soils compared with the soft soils (Fig. 14a). It is also evident that the stiffness of the second layer has more effect on the vibration level compared with the first layers.

7. Safe distance

The results of the parametric analyses were used to develop a safe distance prediction graphs for the historical structures, taking into consideration various types of track systems and different surrounding soil properties. This was made for the five types of historical buildings described in Table 4. A dataset of 1500 allowable distances for various conditions of the track and the surrounding media was created. As a result, contour lines for the safe distance were developed based on the subway structure and the soil types for all the categories of the historical buildings. They are presented in Fig. 15a–e. As illustrated, each graph is composed of a series of distance contours as a function of track type and Impedance Ratio (IR). The impedance ratio is used as an indicator for the soil layers dynamic stiffness [61]. This ratio is a function of the layer density and the shear wave velocity which is described in Eq. (3), where ρ_1 and ρ_2 are the density of the first (top) and the second (underneath) soil layers and v_{s1} and v_{s2} are the shear wave velocity of the first and the second layer, respectively [61].

$$IR = \frac{\rho_2 v_{s2}}{\rho_1 v_{s1}} \tag{3}$$

As indicated in Fig. 15a, the allowable radial distance for class I of historical buildings in various conditions of subway structures and soil types is between 5 and 21 m. As the track stiffness increases, the vibrations are intensified and in turn, the allowable distance is increased. A constant trend could not be seen for impedance ratio of the soil media. When the impedance ratio is less than 1 (i.e., the underneath layer is softer than the top layer), the allowable distances is highly dependent on the impedance ratio. This can be due to two different effects of the soft soil layer which amplifies or reduces the vibration level depending on the wave and soil layer characteristics. The allowable distance from class II of historical buildings for versus soils and subway structure types varies from 4 to 82 m.

8. Application and effectiveness of the results

In order to investigate the effectiveness of the safe distance model (graphs), it was used in the design of the first line of Isfahan metro (Section II) which is adjacent to several historical structures (described in [1]). The SD graphs were used to choose the most appropriate track superstructure system among the four possible types available to the metro (i.e., DFT, FST-MH, FST-ML and HRF). The aim was to ensure that the monumental buildings are in a safe distance. The soil media properties, the CHS type and the track system are presented in Table 8. The CHS types are in Classes *I*, *II* and *III* (as defined in Table 4). Soil properties for each of structure types and radial distance of each structure from tunnel invert are summarized in Table 8. The allowable distance was computed for each track system based on the graphs. As indicated in Table 8, the HRF is the only track system which ensures

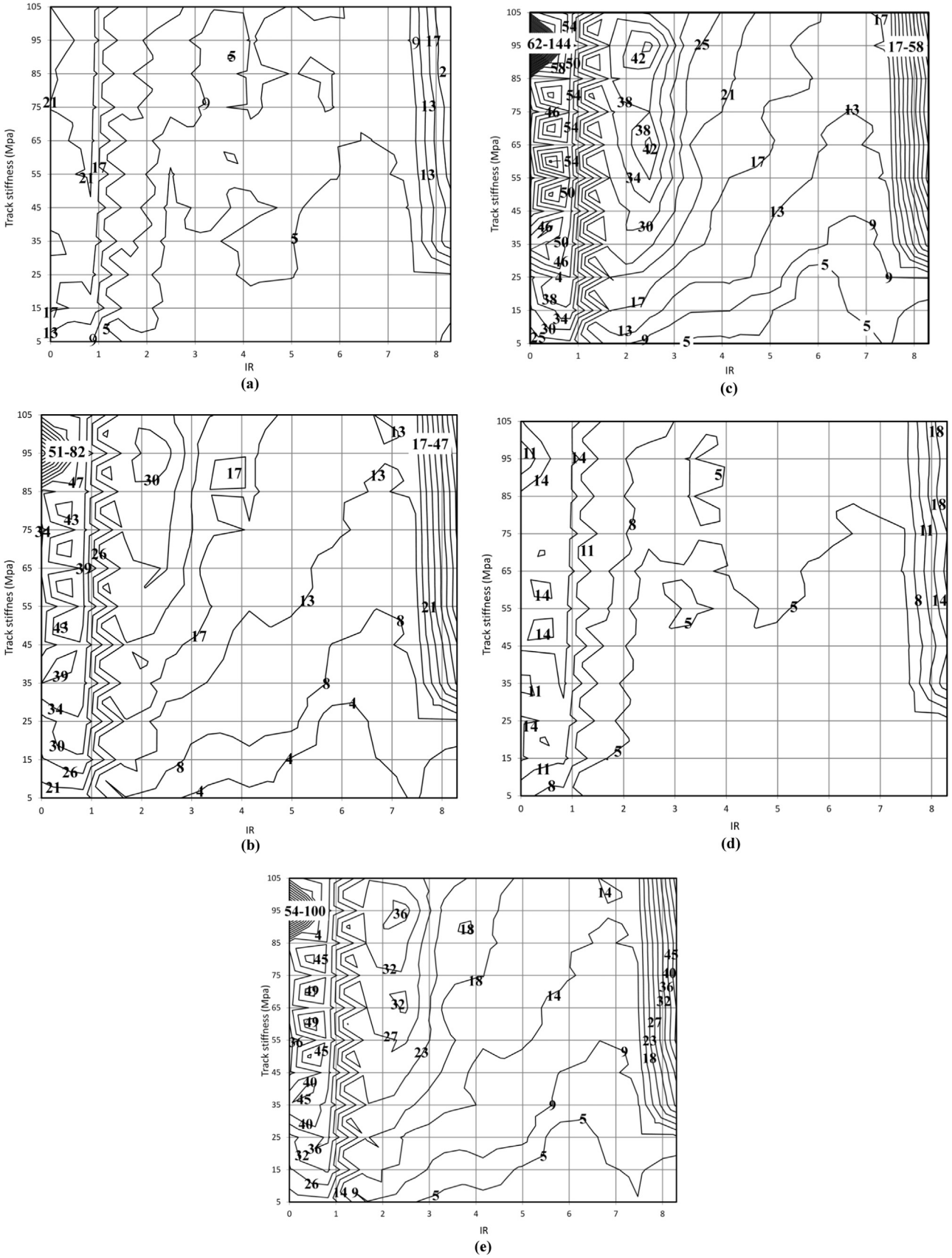

Fig. 15. Safe distance contour for five class of historical and old structures (a) Type I, (b) Type II, (c) Type III (d) Type IV (e) Type V.

Table 8
Results obtained from various possible designs.

Monument		Soil property					Distance from tunnelinvert	Subway Superstructure System (Table 3)	Safe radial Distance From track centerline (m)	Results (S: satisfied NS: not satisfied)
Name	Category from Table 4	Vs1	Vs2	ρ_2	ρ_1	IR				
MCH	III	200	260	21	24	2.2	26	DFT-RP3	**38**	**NS**
								FST-ML	**9**	**S**
								FST-MH	**15**	**S**
								HRF	**9**	**S**
SKH	I	340	450	22	23	1.8	15	DFT-RP3	**13**	**S**
								FST-ML	**5**	**S**
								FST-MH	**7**	**S**
								HRF	**5**	**S**
SSP	II	150	180	23	25	3	8	DFT-RP3	**21**	**NS**
								FST-ML	**4**	**S**
								FST-MH	**6**	**NS**
								HRF	**4**	**S**

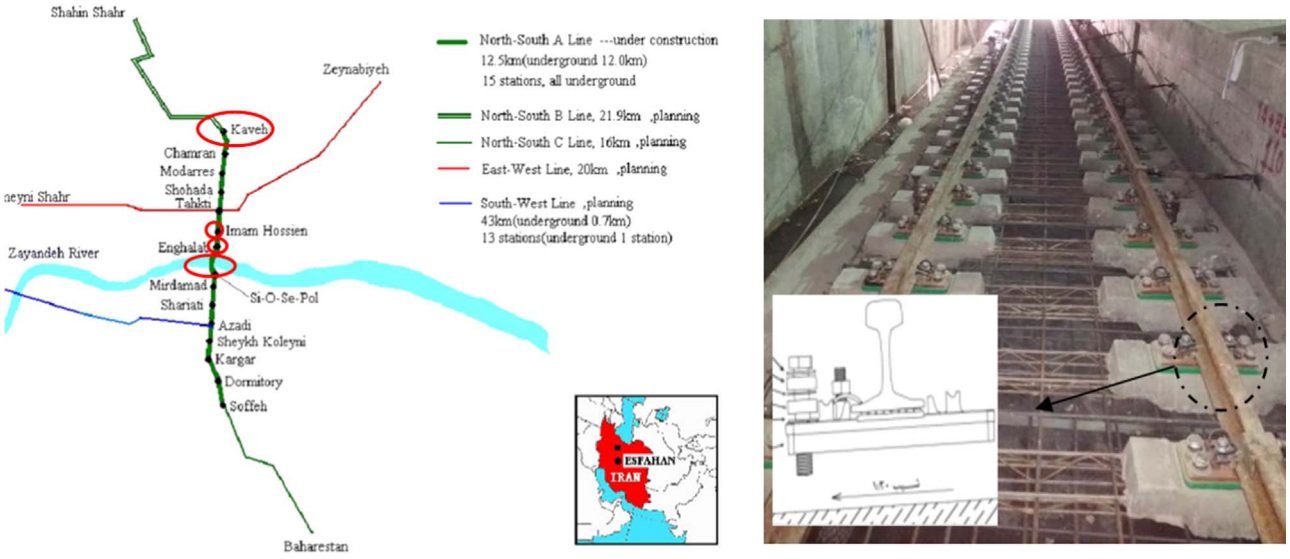

Fig. 16. Subway superstructure system (HRF) designed for Section 2 of Line 1 (Isfahan metro); currently under construction.

the safety of the adjacent historical structures. As a result, a slab track with High Resilient Fastening system (HRF in Table 2) was chosen as a suitable system. This system was proposed to the Isfahan metro authorities and its now under construction (Fig. 16).

9. Conclusions

Construction and operation of underground railway systems (metros/subways) in the historical sites have been one of the main concerns of the world heritage protection bodies such as UNESCO. This is mainly due to the metro ground-borne vibrations. In one hand, metros ease condenses traffic conditions in cosmopolitan cities and boost the tourism industry; on the other hand, there is possibility of serious damages to the cultural and historical structures (CHS) by the metro induced vibrations. The importance and the extent of metro damages to the CHS were illustrated in this research by the evaluations of the results of a prior filed investigation in one of the historical cities. Although there have been various studies into the vibration characteristics of the metros and several measures have been set for the protections of the CHS by the railway industries, these is still a lack of sufficient investigations into the methods or measures by which a metro safe distance from CHSs can be derived.

In response to this need, a thorough theoretical and experimental investigation was made in this research, aimed at developing a safe distance prediction model (in a form of practicable graphs) by which the required minimum metro distances from CHSs can be derived. To develop the prediction graphs, first, the subway structural systems, the surrounding soil media, and the CHS types were categorized into certain categories; second, a finite element model of the track and the surrounding media was developed. The theoretical model was validated by comparisons of its results with those of a comprehensive field measurement carried out in this research. Third, a parametric analysis were made to investigate the effect of the track and surrounding soil parameters on the level of vibrations received by various types of CHS. Using the analyses results, the prediction graphs were developed as a function of the metro characteristics, the geo-mechanical properties of the media between the CHS and the metro, and the CHS types.

In this research, the current track modeling techniques were improved by taking into account the real (in situ) train loading conditions; new classifications of historical buildings and track systems

were developed based on train induced vibrations; and more importantly, a new predication model (in form of graphs) was developed by which the safe distance of CHSs from metros can be derived. The results obtained provide a better understanding of the influences of subway structural characteristics, properties of the surrounding soil media, and the type of CHSs on the vibrations received by the CHSs. The effectiveness and practicability of the graphs/models in construction of new subway lines were illustrated by applying the graphs in the design of a subway system in a historical city. It was shown that the SD graphs developed here is an effective tool for the design of subway lines in the historical cities.

Acknowledgement

This research would have not been possible without the comprehensive technical support of Tehran Urban and Suburban Railway Company, Isfahan Urban and Suburban Railway Company, Tabriz Urban and Suburban Railway Company and Iran Cultural Heritage, Handcraft and Tourism Organization. The authors acknowledge with deep appreciation their untiring support, so vital to the completion of this research. This appreciation is extended to all the enthusiastic and hardworking site engineers and technicians who so carefully carried out all the site activities.

References

[1] ICHTO. Investigation on Possible Damages of Construction and Operation of Isfahan Metro to Adjacent Monumental Structures. Research conucted by IUST, released by Iran cultural Heritage, Handcraft and tourism organization, Research Report - No. 2010. 2011.
[2] Connolly DP, Marecki GP, Kouroussis G, Thalassinakis I, Woodward PK. The growth of railway ground vibration problems—a review. Sci Total Environ 2015.
[3] ITA. Examples of benefits of underground urban public transportation systems. ITA working group on costs-benefits of underground urban public transportation. Tunnelling and underground space technology, 5(1/2). 1990. 2(1), 5–54.
[4] UITP. Getting public transport back on track. PTI Magazine 1/2015, The International Association of Public Transport, UITP. 1. 2015.
[5] Assari A, Assari E. Urban spirit and heritage conservation problems: case study Isfahan city in Iran. J Am Sci 2012;8(1), [202-109].
[6] Clemente P, Rinaldis D. Protection of a monumental building against traffic-induced vibrations. Soil Dyn Earthq Eng 1998;17(5):289–96.
[7] Pau A, Vestroni F. Vibration assessment and structural monitoring of the Basilica of Maxentius in Rome. Mech Syst Signal Process 2013;41(1):454–66.
[8] Wu C, Hao H. Modeling of simultaneous ground shock and airblast pressure on nearby structures from surface explosions. Int J Impact Eng 2005;31(6):699–717.
[9] Singh P, Roy M. Damage to surface structures due to blast vibration. Int J Rock Mech Min Sci 2010;47(6):949–61.
[10] Hao H, Ang T, Shen J. Building vibration to traffic-induced ground motion. Build Environ 2001;36(3):321–36.
[11] Al-Hunaidi M, Rainer J, Tremblay M. Control of traffic-induced vibration in buildings using vehicle suspension systems. Soil Dyn Earthq Eng 1996;15(4):245–54.
[12] Hao H, Ang TC. Analytical modeling of traffic-induced ground vibrations. J Eng Mech 1998;124(8):921–8.
[13] Athanasopoulos G, Pelekis P. Ground vibrations from sheetpile driving in urban environment: measurements, analysis and effects on buildings and occupants. Soil Dyn Earthq Eng 2000;19(5):371–87.
[14] Vogiatzis C. Vibration at buildings of high cultural value from TBM operation at Athens metro line: Akademia-Syntagma. Inter-noise and noise-con congress and conference proceedings. Institute of Noise Control Engineering. 2000.
[15] Crispino M, D'apuzzo M. Measurement and prediction of traffic-induced vibrations in a heritage building. J Sound Vib 2001;246(2):319–35.
[16] Watts G. Traffic induced vibrations in buildings. Transport and Road Research Laboratory (TRRL), Report No. 46. 1990.
[17] Whiffin A, Leonard D. A survey of traffic induced vibrations. Transport and Road Research Laboratory (TRRL), Report/Paper Numbers No Lr418. 1971.
[18] Augenti N, Clemente P. Strength reduction in masonry due to dynamic loads. Proceedings, IABSE symposium extending the lifespan of structures. 1995.
[19] Ma M, Liu W, Qian C, Deng G, Li Y. Study of the train-induced vibration impact on a historic Bell Tower above two spatially overlapping metro lines. Soil Dyn Earthq Eng 2016;81:58–74.
[20] Hanson Carl E, Towers David A, Meister Lance D. Transit noise and vibration impact assessment. No. FTA-VA-90-1003-06; 2006.
[21] Vogiatzis K. Environmental ground borne noise and vibration protection of sensitive cultural receptors along the Athens Metro Extension to Piraeus. Sci Total Environ 2012;439:230–7.
[22] Vogiatzis K, Kouroussis G. Prediction and efficient control of vibration mitigation using floating slabs: practical application at Athens metro lines 2 and 3. Int J Rail Transp 2015;3(4):215–32.
[23] Cox S, Wang A. Effect of track stiffness on vibration levels in railway tunnels. J Sound Vib 2003;267(3):565–73.
[24] Mitra S, Grover A, Sing R. Handbook of conservation of heritage buildings. Nirman Bhawan, New Delhi: Directorate General, Central Public Works Department, 101 A; 2013, [110011].
[25] GB/T50452 . Technical specifications for protection of historic buildings against man-made vibration. Beijing: China building industry press; 2008.
[26] Monti G, Fumagalli F, Marano G, Quaranta G, Rea R, Nazzaro B. Effects of ambient vibrations on heritage buildings: overview and wireless dynamic monitoring application. Proceedings of the 3rd international workshop dynamic interaction of soil and structures-dynamic interaction between soil, monuments and built environment (DISS 2013). Rome, Italy; 2013.
[27] Verbraken H, Degrande G, Lombaert G, Stallaert B, Cuéllar V. Benchmark tests for soil properties, including recommendations for standards and guidelines. RIVAS project SCP0-GA-2010-265754, Deliverable D1. 2013.
[28] Pichler D, Zindler R. Development of artificial elastomers and application to vibration attenuating measures for modern railway superstructures. Proceedings of the first European conference on constitutive models for rubber. 1999.
[29] Sunley V, Cox S. Pandrol vanguard on London underground. In: Railway infrastructure. 2001. 99–105.
[30] Wagner HG. Attenuation of transmission of vibrations and ground-borne noise by means of steel spring supported low-tuned floating track-beds. 2002 world metro symposium, Taipei; 2002.
[31] Dorfner TH. Designed elasticity for railway superstructures-system design aspects and typical components. Noise-con 04. The 2004 National conference on noise control engineering. 2004.
[32] Cox S, Wang A, Morison C, Carels P, Kelly R, Bewes O. A test rig to investigate slab track structures for controlling ground vibration. J Sound Vib 2006;293(3):901–9.
[33] Kramer SL. Geotechnical earthquake engineering. Pearson Education India; 1996.
[34] Merritt FS. Minimum design loads for buildings and other structures: American society of civil engineers standard 7-95. J Arch Eng 1996;2:80–1.
[35] Eurocode CEN 1998-1. Design of structures for earthquake resistance—part 1: general rules, seismic actions and rules for buildings (EN 1998-1: 2004). European Committee for Normalization, Brussels; 2004.
[36] FEMA450 . NEHRP recommended provisions for seismic regulations for new buildings and other structures. (FEMA450): Provisions, Building Seismic Safety Council, National Institute of Building Sciences; 2004.
[37] López MD, Romero A, Connolly DP, Galvín P. Scoping assessment of building vibration induced by railway traffic. Soil Dyn Earthq Eng 2017;93:147–61.
[38] DIN4150 . Vibrations in building construction, institute of environmental sciences, considerations in clean room design. German Standards Organization; 1970.
[39] Rainer J. Effect of vibrations on historic buildings, XIV. The Association for Preservation Technology Bulletin; 1982. p. 2–10.
[40] Konon W, Schuring JR. Vibration criteria for historic buildings. J Constr Eng Manag 1985;111(3):208–15.
[41] BS7385-1. Evaluation and measurement for vibration in building: part 1: guide for measurement of vibrations an evaluation of their effects on buildings. London; 1990.
[42] BS7385-2. Evaluation and measurement for vibration in building: part 2: guide to damage levels from ground borne vibration. London; 1993.
[43] Jones S. Transportation and construction-induced vibration guidance manual. Sacramento, Calif: Calif Department of Transport, Noise, Vibration, and Hazardous Waste Management Office; 2004.
[44] Connolly DP, Kouroussis G, Giannopoulos A, Verlinden O, Woodward PK, Forde MC. Assessment of railway vibrations using an efficient scoping model. Soil Dyn Earthq Eng 2014;58(0):37–47.
[45] Kouroussis G, Connolly DP, Alexandrou G, Vogiatzis K. The effect of railway local irregularities on ground vibration. Transp Res Part D: Transp Environ 2015;39:17–30.
[46] Connolly DP, Giannopoulos A, Forde M. Numerical modelling of ground borne vibrations from high speed rail lines on embankments. Soil Dyn Earthq Eng 2013;46:13–9.
[47] Rayleigh J, Lindsay RB. The theory of sound, Unabridged Second Revised edition, 1. Dover Publications; 1945.
[48] Leger P, Ide IM, Paultre P. Multiple-support seismic analysis of large structures. Comput Struct 1990;36(6):1153–8.
[49] Nsabimana E, Jung YH. Dynamic subsoil responses of a stiff concrete slab track subjected to various train speeds: a critical velocity perspective. Comput Geotech 2015;69:7–21.
[50] Nejati HR, Ahmadi M, Hashemolhosseini H. Numerical analysis of ground surface vibration induced by underground train movement. Tunn Undergr Space Technol 2012;29:1–9.
[51] Lysmer J, Kuhlemeyer RL. Finite-dynamic model for infinite media. J Eng Mech Div 1969;95(4):859–77.
[52] Kouroussis G, Verlinden O, Conti C. Finite-dynamic model for infinite media: corrected solution of viscous boundary efficiency. J Eng Mech 2011;137(7):509–11.
[53] Connolly DP, Costa A, Kouroussis G, Galvin P, Woodward P, Laghrouche O. Large scale international testing of railway ground vibrations across Europe. Soil Dyn Earthq Eng 2015;71:1–12.
[54] Havskov J, Alguacil G. Seismic recorders, instrumentation in earthquake seismology. Springer; 2004. p. 113–49.
[55] Huang H, Agafonov V, Yu H. Molecular electric transducers as motion sensors: a review. Sensors 2013;13(4):4581–97.
[56] Tang G, Yang B, Jq Liu, Xu B, Zhu Hy, Yang CS. Development of high performance

piezoelectric d33 mode MEMS vibration energy harvester based on PMN-PT single crystal thick film. Sens Actuators A: Phys 2014;205:150–5.
[57] Cox S, Wang A, Adedipe A. Survey of metro excitation frequencies and coincidence of different modes. Noise and vibration mitigation for rail transportation systems. Springer; 2008. p. 78–85.
[58] TUSC . Railway track and tunnel system specification for tehran metro line 3-detail design. Tehran Urban and Suburban Company, Behin Saz consulting engineers; 2015.
[59] TUSC . Soil mechanic and fundation studies, X3 and W3 stations. Tehran Urban and Suburban Company, Zamiran consulting engineers submitted to Boland Payeh Co.; 2015.
[60] Kerr AD. Fundamentals of railway track engineering. Simmons-Boardman Publishing Corporation; 2003.
[61] Yang YB, Hung H, Hong X. Wave propagation for train-induced vibrations: a finite/infinite element approach. World Scientific Publishing Company Incorporated; 2009.